Materials Horizons

ROYAL SOCIETY OF CHEMISTRY

COMMUNICATION

View Article Online
View Journal

Cite this: DOI: 10.1039/d5mh02005k

Received 22nd October 2025,
Accepted 26th February 2026

DOI: 10.1039/d5mh02005k

rsc.li/materials-horizons

A strippable catechol-terminated polyurethane coating for large-area radioactive cesium decontamination

Jae Seung Lee, †[a] Ye-won Jeong, †[b] Donghyun Kim, †[a] Hyung-Ju Kim, [bc] Sung-Wook Kim, [c] Hee-Man Yang, *[bc] Myung-Jin Baek *[a] and Dong Woog Lee *[a]

Efficient and rapid decontamination of radioactive elements is important to prevent radioactive exposure. Herein, we develop a strippable catechol-terminated polyurethane (CPU) coating for effective surface decontamination. Our polyurethane coating can be directly applied to contaminated surfaces *via* simple spraying or solution casting, followed by rapid drying at room temperature. The resulting coating is easily stripped off with sufficient toughness and adhesion strength, showing superior ^{137}Cs removal efficiency on stainless steel (~94.9%) and rough cement (~59.1%), in a much shorter time (<3 h) compared to commercial decontamination coatings (~93.8% on stainless steel and ~8.4% on cement after 24 h). This performance can be attributed to the strong adhesion and cohesion mediated by catechol moieties. Furthermore, after use, the coating waste is readily dissolvable in acetone, suggesting potential for reducing radioactive waste with the aid of an appropriate separation process, thereby preventing secondary contamination. These results establish CPU as a promising radioactive decontamination strategy.

New concepts

Strippable coatings have long been used for surface decontamination, but they often rely on irreversible crosslinked polymers that are slow to dry and difficult to recycle. This work introduces a catechol-terminated polyurethane (CPU) coating simultaneously achieving rapid decontamination and dissolvable characteristic after use. By integrating mussel-inspired adhesion chemistry with solvent-responsive polymer design, the CPU coating enables rapid drying and facile sprayable application for large-area treatment, while maintaining high decontamination performance. In addition, the coating can readily dissolve after stripping, providing a potential approach for waste minimization through post-treatment separation. This dual design resolves the long-standing trade-off between short drying time and solvent dissolvability with effective decontamination performance, offering a conceptually new route toward rapid, scalable, and sustainable decontamination materials.

Introduction

The generation of nuclear energy as a low-carbon power source has grown significantly in recent years.[1] However, nuclear accidents, such as those at Chernobyl and Fukushima Daiichi, have demonstrated the catastrophic results of radionuclide release.[2] Among the various radionuclides, cesium-137 (^{137}Cs) is particularly hazardous due to its high fission yield, long half-life (30.2 years), and strong gamma radiation emissions.[3] Its high solubility in water allows it to spread rapidly in the environment,[4] posing significant risks to ecosystems and human health. Consequently, surface decontamination is an important strategy for mitigating environmental and health impacts from nuclear incidents and maintaining the safe operation of nuclear facilities.[5]

Conventional decontamination methods, such as high-pressure washing and abrasive removal, are widely used,[6] but they have notable drawbacks. High-pressure washing generates large volumes of contaminated liquid waste, and abrasive removal often damages surfaces and produces fine particulate waste.[7] Advanced technologies like ionic washing[8] and dry ice blasting[9] have been developed to overcome these issues; however, they still require specialized equipment and involve complex procedures. These challenges emphasize the need for scalable decontamination strategies, minimize secondary waste, prevent substrate damage, and enable rapid and effective performance.

Strippable coatings have emerged as a promising alternative for surface decontamination.[10] These coatings adhere to contaminated surfaces, trapping radioactive contaminants within their matrix, and can be stripped off after drying or curing.[11] Compared to traditional methods, strippable coatings

[a] School of Energy and Chemical Engineering, Ulsan National Institute of Science and Technology (UNIST), 50 UNIST-gil, Ulsan, 44919, Republic of Korea. E-mail: dongwoog.lee@unist.ac.kr, bagmj100@unist.ac.kr
[b] Nuclear Science and Technology, University of Science and Technology (UST), 217, Gajeong-ro, Daejeon, 34113, Republic of Korea
[c] Nuclear Facility Cleanup Technology Division, Korea Atomic Energy Research Institute (KAERI), 989-111 Daedukdaero, Yuseong, Daejeon, 34057, Republic of Korea. E-mail: hmyang@kaeri.re.kr
† Authors with equal contributions to this work.

minimize secondary waste, prevent damage to surfaces, and offer a simple application process. Among various types, UV-curable strippable coatings, such as polyurethane acrylates (PUA),[12] have been employed, due to their flexibility, strong mechanical properties, long-term stability, and rapid curing by UV. Liu *et al.* prepared a UV-cured coating by forming a PUA-crosslinking network. The PUA-crosslinked coating was cured by 1 min of UV irradiation with high decontamination efficiency on various surfaces. However, the permanently cross-linked nature of UV-curable polymers generally limits their solubility after curing, which may result in the generation of secondary organic radioactive waste. In addition, the requirement for UV irradiation can pose practical challenges for large-scale field applications.

To address these limitations, various systems that are dissolvable in a specific solvent have been explored. For instance, Yang *et al.* reported a pH-responsive boronic acid-based self-generating hydrogel coating[13] formed by mixing two liquid components, which is dissolvable in water after use. Although this system successfully reduced secondary organic radioactive waste, the complex 2-category spray application was required. Moreover, its cohesive strength is insufficient for an easy and clean stripping process. Another example, a commercial product, DeconGel, has notable limitations, including slow drying time (~24 h, according to the product description), poor removal efficiency for porous surfaces like cement,[14] degradation in wet environments, and low adhesion, as illustrated in Fig. 1a. Therefore, the development of advanced decontamination methods with minimized waste, facile process, strong adhesion, and enhanced removal efficiency is highly desired.

To achieve both enhanced adhesion to contaminated surfaces and improved removal efficiency of radionuclides, inspired by mussel adhesion chemistry, we hypothesized that catechol termination could simultaneously enhance interfacial adhesion and cohesive integrity. Catechol, observed in mussel adhesive proteins,[15] is well-known for its superior adhesion to a variety of surfaces and high cohesion properties through interactions such as hydrogen bonding,[16] π–π interaction,[17] cation-π interaction,[18] and metal coordination.[19] These versatile interactions can induce a mechanically robust coating with strong adhesion properties.[20]

In this study, we present a strippable catechol-terminated polyurethane (CPU) coating for a facile and efficient radioactive decontamination method, as illustrated in Fig. 1b. The CPU coating also enables rapid application and drying, while remaining readily dissolvable after use for potential recycling. The terminal catechol groups enhanced the mechanical toughness and adhesive strength of the CPU, surpassing those of the alkyl-terminated polyurethane (APU) coating. Moreover, the CPU coating exhibited a superior Cs^+ removal efficiency on stainless steel (~94.9%) and cement (~59.1%) compared to DeconGel (~93.8% and ~8.4%, respectively), even after a significantly shorter drying time (3 h *vs.* 24 h). Since the coating can be applied using portable spray equipment, it is a promising candidate for wide-area decontamination in nuclear facilities decommissioning,[21] protection against chemical warfare agents,[22] and heavy metal removal (Fig. 1c).[23]

Results and discussion

Preparation and characterization of strippable polyurethane (PU) coatings

Strippable PU coatings were prepared by two-step polymerization. The H_6XDI-terminated PU prepolymer was polymerized by polycaprolactone diol (PCL) and H_6XDI. CPU was synthesized by reacting dopamine hydrochloride with the PU prepolymer, as illustrated in Fig. S1. To investigate the effect of terminal catechol groups, we compared CPU with APU as a control (Fig. 2a). APU was synthesized by reacting ethanol with the PU prepolymer. The synthesized PUs were characterized using FT-IR (Fig. 2b) and ^{1}H-NMR spectroscopies (Fig. S2 and S3). FT-IR spectra displayed the disappearance of NCO group peak at 2250 cm^{-1}, indicating the complete polymerization. The FT-IR peaks corresponding to the C=C stretching of benzene rings at 1670 cm^{-1}, and distinct ^{1}H-NMR peaks for benzene groups (6.5–7.0 ppm), resulting from the aromatic groups of the catechol, further verified the successful synthesis of CPU.

Generally, PCL-based PUs are reported as semi-crystalline polymers, exhibiting a crystalline peak near their crystallization temperature.[24] The normal X-ray diffraction (XRD) results confirmed the semi-crystalline structure of both CPU and APU,

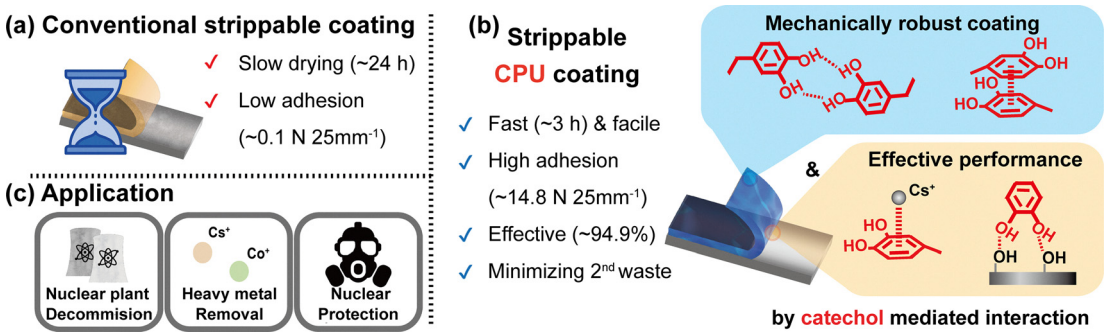

Fig. 1 Illustration and the characteristics of strippable coatings, including (a) the conventional strippable coating, (b) the developed strippable catechol-terminated polyurethane coating (CPU), and (c) possible area of application.

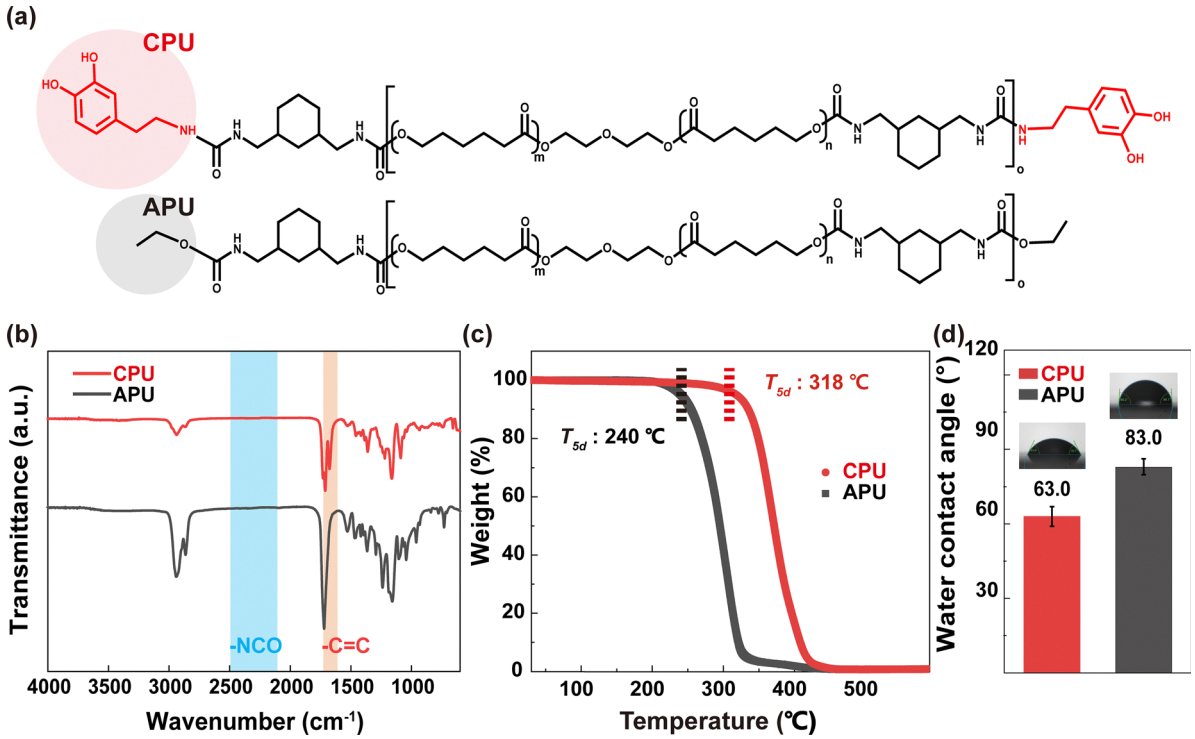

Fig. 2 Characterization of strippable catechol-terminated (CPU) and alkyl-terminated (APU) polyurethane coatings. (a) Molecular structure of strippable CPU and APU. (b) FT-IR curves of CPU and APU. (c) TGA curves of CPU and APU. (d) Water contact angle measurements of CPU and APU.

with crystalline peaks observed at (110) and (200) lattice planes (Fig. S4). The crystallization temperature (T_c) and melting temperature (T_m) of the PUs were measured using DSC (Fig. S5). Consistent with the XRD results, CPU exhibited weak crystallinity. This crystallinity peak of CPU in DSC is thought to result from microphase separation of the polymer induced by catechol-mediated hydrogen bonding.[25] DSC also revealed that CPU had a higher T_m (39.7 °C) compared to APU (35.6 °C). The thermal degradation behavior of PUs was analyzed *via* TGA. A 5% weight loss temperature (T_{5d}) was higher for CPU (318 °C) compared to APU (240 °C), indicating sufficient thermal stability for general applications (Fig. 2c and Table S1). The higher T_m and T_{5d} values of CPU compared to APU can be attributed to the hydrogen bonding,[26] which occurs between catechol terminal groups[27] as well as between catechol and ether groups.[28] The higher hydrogen bonding of CPU can also contribute to its higher storage modulus, measured using a rheometer, ensuring adequate rigidity for strippable coatings (Fig. S6).

To optimize the strippable coating solution, the polymer content was optimized to achieve an appropriate viscosity for spray applications (Table S2). Samples with excessively low solid content led to sagging or splattering during spraying,[29] whereas those with overly high solid content exhibited too high viscosities, low processability, and nozzle clogging.[30] Therefore, a solid content of 20 wt% (20 CPU), which exhibited appropriate viscosity for spraying (0.76 Pa s^{-1} at a shear rate of 1000 s^{-1}), was selected as the optimal concentration.

The polymer samples were prepared using a H_2O/acetone mixture. To optimize solvent composition, the polymer solution was prepared with varying water contents (0–25 wt% H_2O/acetone), as summarized in Table S3 and Fig. S7. The water contents simultaneously affect the dispersion stability of the solution, the dissolution rate of the radioactive contaminants such as Cs^+,[31] and drying time. In terms of dispersion stability, CPU maintained a clear single-phase solution up to 15 wt% H_2O, while a yellowish dispersion was observed at 20 wt%, followed by phase separation at 25 wt%. In contrast, APU exhibited cloudy dispersions at H_2O contents above 15 wt%, followed by phase separation at 25 wt%.[32] The higher water solubility and hydrophilicity of CPU (as shown in Fig. 2d) compared to APU can be attributed to the presence of catechol moieties, which contain two adjacent hydroxyl groups capable of forming strong hydrogen bonds with water molecules.[33] To investigate the effects of water content and drying time on adhesion and decontamination performance, the water content in the CPU and APU coatings was adjusted to achieve different drying times: 10 wt% H_2O yielded a drying time of 1 h, while 20 wt% H_2O resulted in a drying time of 3 h.

Mechanical and adhesive properties of strippable PU coatings

Strippable coatings should possess good mechanical properties to resist physical damage.[34] In particular, they require high tensile strength and toughness to withstand external forces, as well as sufficient flexibility to prevent tearing or breaking during stripping. The inherent flexibility and mechanical robustness of polyurethanes (PUs) make them highly suitable for strippable coating applications.[35,36] CPU exhibited strong and tough mechanical properties by strong hydrogen bonding

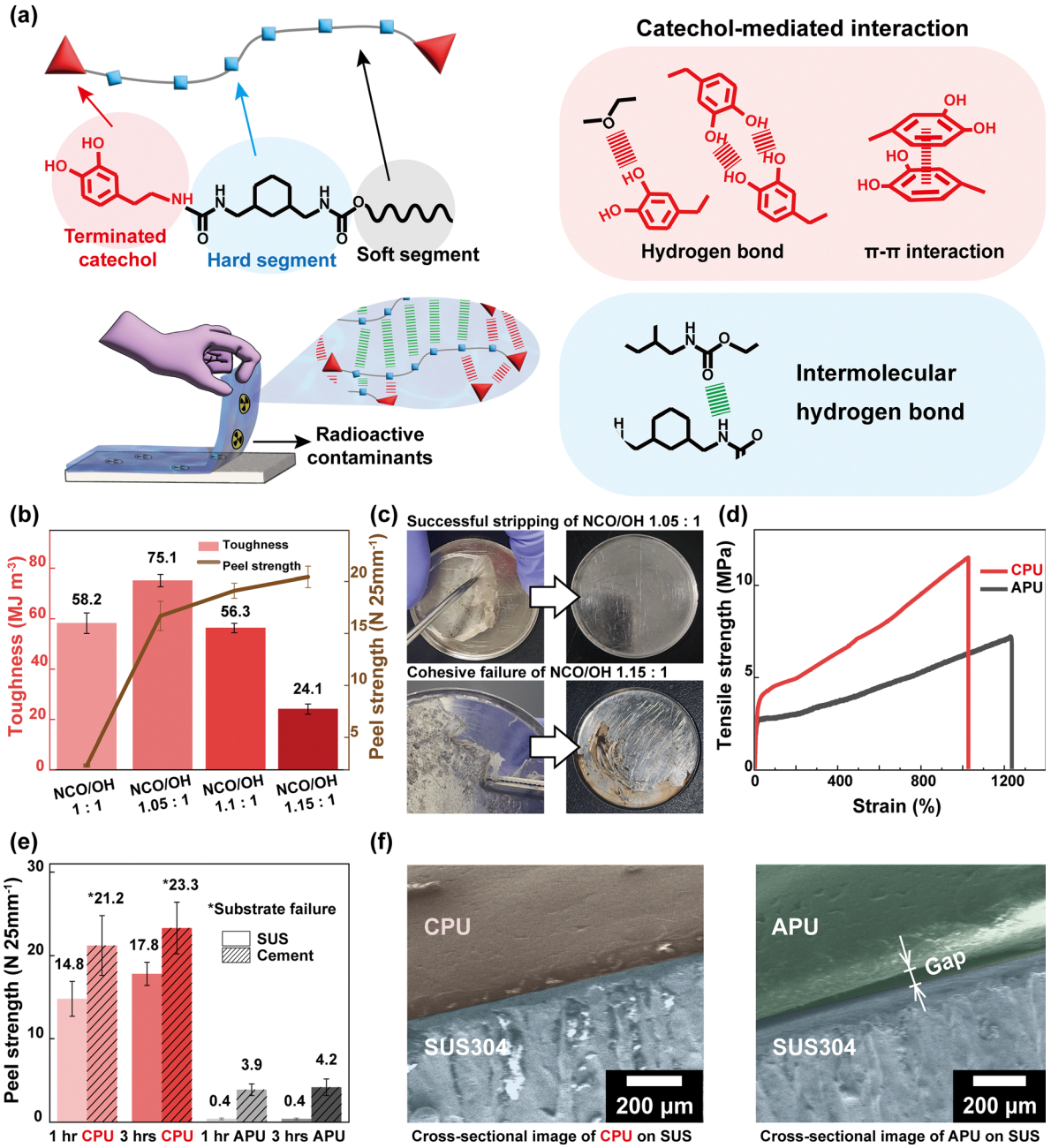

Fig. 3 Mechanical and adhesive properties of strippable PU coatings. (a) Schematic illustration of catechol-mediated intermolecular interactions. (b) Toughness and peel strength of CPU samples with varying NCO/OH ratios. (c) Representative images of successful stripping of PU with an NCO/OH ratio of 1.05 : 1, and cohesive failure for PU with a ratio of 1.15 : 1. (d) Stress–strain curve of PU with an NCO/OH ratio of 1.05 : 1 PUs. (e) Peel strength of PU coatings in various substrates and drying times. (f) Cross-sectional SEM images showing the interface between the stainless steel (SUS) surface and the PU coatings.

mediated by catechol groups. Catechol groups can participate in hydrogen bonding, π–π interactions with other catechol moieties,[37] and additional hydrogen bonding with ether groups.[28] In contrast, APU exhibited relatively low mechanical strength due to the presence of hydrogen bonding only between urethane segments (Fig. 3a).[38]

To optimize the mechanical and adhesive properties of the strippable polyurethane (PU) coating, a series of polymers were synthesized by varying the NCO/OH molar ratio from 1 : 1 to 1.15 : 1, corresponding to catechol/PCL feed ratios ranging from 0 to 30 mol% (Tables S4 and S5). Increasing the NCO/OH ratio led to a reduction in both the molecular weight and degree of polymerization (DP), while simultaneously increasing the feed ratio of terminal catechol groups. Based on the DP, the polymer prepared with an NCO/OH ratio of 1.05 : 1 was composed of 14.8 repeating units and two catechol terminal groups. Polymers with higher NCO/OH ratios exhibited increased adhesive strength but reduced mechanical performance, often resulting in cohesive failure during peeling. This trade-off was attributed to their lower molecular weight and weaker intermolecular interactions.[39]

As shown in Fig. 3b and c, the polymer with an NCO/OH ratio of 1.05 : 1 achieved an optimal balance, exhibiting strong adhesion without cohesive failure. In contrast, the weak mechanical properties and cohesive failure observed in CPU (NCO/OH 1.15 : 1) led to residual contaminants and coating remnants on the surface, thereby reducing decontamination performance. These results indicate that the optimal catechol content can enhance both the toughness and adhesive strength of the polymer. Based on this finding, CPU was optimized at an NCO/OH ratio of 1.05 : 1 with a catechol content of 0.1 mol%. Similarly, APU was synthesized with the same NCO/OH ratio (1.05 : 1) and an alkyl content of 0.1 mol%.

A Universal Testing Machine (UTM) was used to investigate the effects of catechol groups in CPU, compared to APU, on their mechanical properties and adhesive strength. CPU exhibited higher tensile strength (12.2 MPa) and toughness (75.1 MJ m^{-3}) than APU (9.0 MPa and 70.7 MJ m^{-3}, respectively) (Fig. 3c and Table S6).

The adhesive properties of strippable coatings are critical for preventing unintended detachment caused by external factors which can compromise decontamination efficiency.[40] However, when adhesion strength exceeds the internal cohesion of the coating, cohesive failure can occur, leaving residues on the surface, diminishing decontamination performance and requiring an excessive force during stripping, ultimately reducing usability.[41] To achieve residue-free decontamination, strippable coatings should be engineered to possess high internal cohesion and a well-balanced level of adhesion strength.

Adhesion performance under different stress conditions was assessed using lap shear and 180° peel tests. The lap shear test measures adhesive strength under shear stress, which is influenced by both interfacial adhesion and cohesive integrity.[42] The 3 h CPU sample exhibited significantly higher lap shear strength (15.7 kPa) compared to APU (~0.1 kPa) (Table S6), indicating strong interfacial adhesion with the substrate and high cohesive strength within the coating.

Since strippable coatings may commonly be applied to both equipment and building surfaces,[10] it is essential to evaluate their adhesion performance on representative materials. SUS and cement were selected as test substrates, and 180° peel tests were performed after 1 and 3 h of drying to examine the effects of substrate type and drying time on adhesion (Fig. 3e).

On SUS, CPU exhibited increased peel strength with longer drying time (14.8 N 25 mm^{-1} for 1 h CPU and 17.8 N 25 mm^{-1} for 3 h CPU), which is attributed to an increase in real contact area and polymer chain rearrangement at the interface. This rearrangement promotes catechol group exposure on the surface, thereby enhancing interfacial adhesion.[43] On cement, peel strengths were generally higher than those on SUS, with comparable values observed for 1 h (21.2 N 25 mm^{-1}) and 3 h (23.3 N 25 mm^{-1}) CPU. These results were attributed to substrate failure in both cases. Notably, 3 h CPU caused more severe surface damage to the cement, likely due to deeper polymer penetration into the porous substrate during the extended drying period. The enhanced adhesion on cement compared to SUS is primarily due to mechanical interlocking within the porous cement matrix.[44] In contrast, APU exhibited significantly lower peel strength on SUS (~0.4 N 25 mm^{-1}) and cement (~4 N 25 mm^{-1}), compared to CPU.

To visualize the interface between the coatings and the SUS surfaces, cross-sectional scanning electron microscopy (SEM) was performed. As shown in Fig. 3f, the SEM images revealed distinct differences at the interface between SUS and the coatings. The highly adhesive CPU coating maintained intimate contact with the surface through catechol-mediated interactions, which enhanced interfacial adhesion and prevented unintended detachment. In contrast, the APU coating frequently exhibited noticeable interfacial gaps. Although the APU polymer contains ester groups that can contribute to interfacial interactions, the absence of catechol moieties resulted in weak adhesion to SUS, thereby leading to partial microscopic detachment.

^{137}Cs removal performance by the strippable PU coatings

The removal of fallout particles should be considered a key performance indicator for evaluating the effectiveness of strippable coatings.[45] Fallout is generated by the intense heat produced during nuclear fission, which vaporizes various elements at the detonation site. Upon condensation, these vapors form particulate matter containing both radioactive metallic elements and common components from surrounding materials such as concrete and soil. To simulate real fallout contamination, a simulated fallout (SFO) was prepared, containing cesium (Cs), strontium (Sr), cobalt (Co), and silicon (Si).[46] SFO was applied to SUS by scattering the particles, followed by the addition and evaporation of water to create a uniformly contaminated surface. The applied SFO can exist in both particulate and ionic forms, and it is important to evaluate the removal efficiency for each species. In their particulate forms, fallout can be easily dispersed into the air, posing serious health risks such as lung cancer.[47] Additionally, Cs, Sr, and Co in fallout readily dissolve and ionize in water.[48] In their ionized forms, these elements can spread through water systems, including rivers and drinking water, thereby entering both ecosystems and the human body.[49] Accordingly, SFO tests were designed to assess the removal of ion-containing particles, simulating realistic fallout contamination scenarios.

To evaluate the SFO decontamination performance of CPU and APU, their removal capabilities were compared with that of DeconGel, a commercially available strippable coating. DeconGel was selected as a reference material due to its well-documented efficacy in nuclear decontamination applications.

Firstly, SEM was used to directly observe residual particulate contaminants on SUS substrates after stripping. As shown in Fig. 4a, both CPU and APU successfully removed SFO contaminants within 3 h, leaving no visible residues. This performance is comparable to that of DeconGel after 24 h of application.

Secondly, the removal performance of Cs^{+}, Sr^{2+}, and Co^{3+} ions from SFO was measured by UV-Vis spectroscopy (Fig. 4b and Table S7).[50] Under 1 h drying conditions, CPU showed higher removal efficiency (90.3%) compared to APU (83.7%). After 3 h of drying, both coatings exhibited improved performance, with 3 h CPU achieving 97.5% removal and 3 h APU reaching 94.7%. For the quantitative assessment of individual

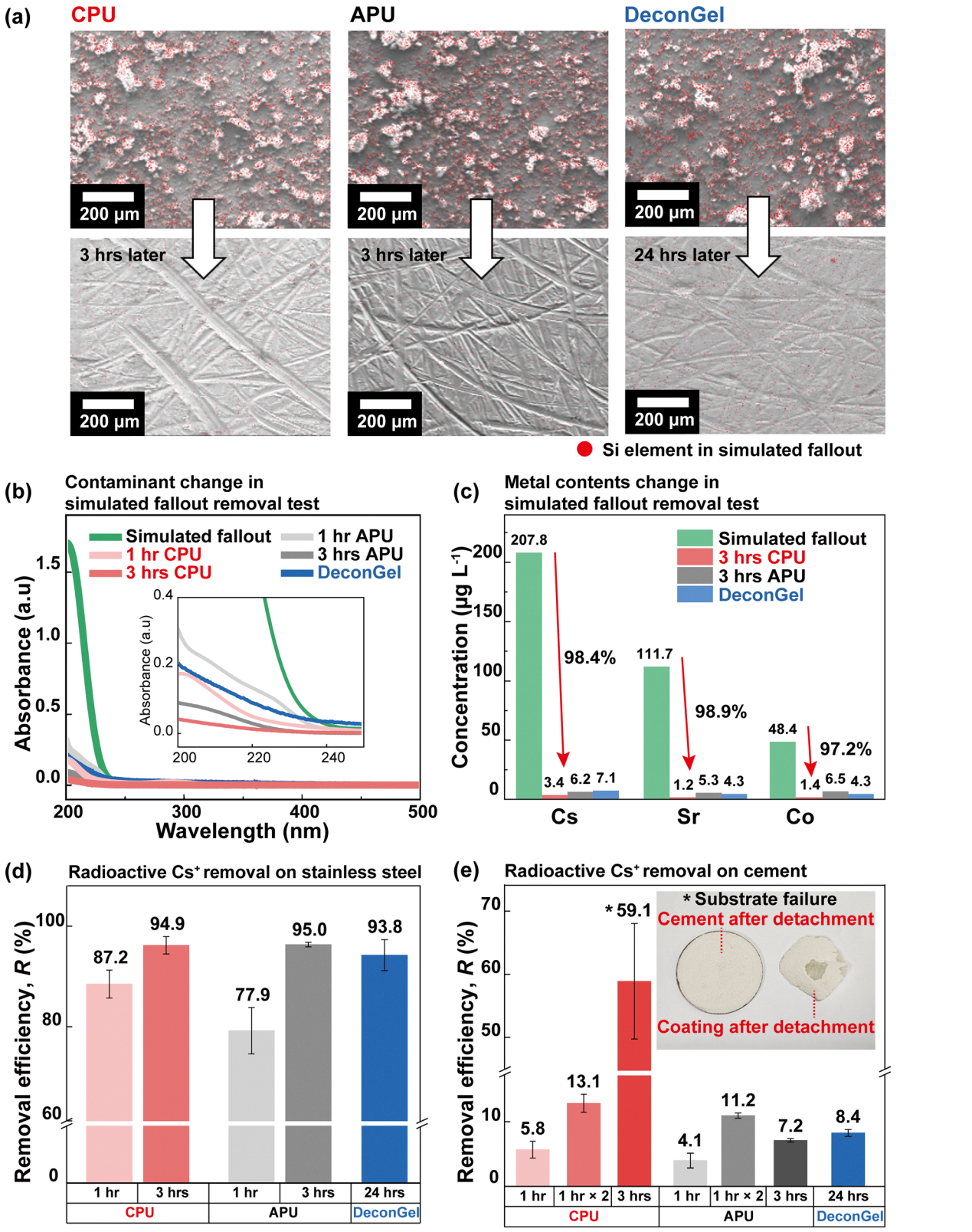

Fig. 4 Decontamination performances of strippable coatings. (a) SEM images of SUS before and after decontamination by CPU, APU, and DeconGel in the simulated fallout (SFO) test. (b) UV-Vis spectroscopy before and after decontamination, and (c) metal concentration measurements by ICP-TQ-MS in the SFO test. (d) Removal efficiency on SUS, and (e) rough cement substrates in the radioactive isotope (RI) test.

ion removal, ICP-TQ-MS was used to analyze elemental concentrations in solution before and after decontamination (Fig. 4c and Table S8). The results confirmed that CPU achieved excellent removal efficiencies across all tested ions: 98.4% for Cs^+, 98.9% for Sr^{2+}, and 97.2% for Co^{3+}.

Considering the combined results from UV-Vis and ICP-TQ-MS analyses, 1 h CPU demonstrated superior decontamination efficiency compared to 1 h APU. To elucidate the underlying interaction mechanisms responsible for the distinct decontamination performances of CPU and APU coatings, X-ray photoelectron spectroscopy (XPS) was employed to investigate the role of the catechol moiety in Cs^+ removal (Fig. S8). After decontamination, the Cs 3d signal appeared in the high-resolution XPS spectra. The peaks at 738.7 eV and 724.8 eV corresponded to Cs $3d_{3/2}$ and Cs $3d_{5/2}$, respectively.[54] The presence of these peaks confirmed the retention of Cs species within both PU coatings after decontamination. In the O 1s spectrum, the CPU exhibited an additional component at 531.7 eV, which was attributed to the Cs–O interaction.[55] The emergence of a Cs–O region is related to catechol hydroxyl groups, suggesting a preferential association of Cs^+ with catechol-containing domains. In contrast, APU did not show a distinct Cs–O peak and only C═O and C–O peaks shifted to the higher binding energy, indicating that Cs^+ primarily interacts with carbonyl or ether oxygen sites in APU. This resulted in a significant difference in decontamination efficiency under the 1 h drying condition. Also, the enhanced decontamination performance of CPU is attributed to CPU's higher hydrophilicity (Fig. 2d), which promotes faster ion diffusion and stronger interaction with the coating matrix. Such rapid ion-capturing capability renders 1 h CPU particularly advantageous for urgent radioactive decontamination tasks. However, as physical encapsulation became more dominant over time, the efficiency difference between APU and CPU decreased.

Moreover, the radioactive decontamination performance was evaluated using radioactive isotope (RI) tests by comparing the ^{137}Cs radiation levels before and after treatment. The tests were conducted on two substrates: SUS, widely utilized in equipment and construction materials, and cement, characterized by its rough structure and used in building applications (Fig. 4d and e). The surface morphology of the cement was analyzed using a confocal optical profiler (Fig. S9). The surface roughness (R_a) was measured to be approximately 13 μm, which corresponds to that of a typical exterior wall cement surface prepared by sandblasting.[51] The removal efficiency R was calculated using eqn (1):[52]

$$R = \frac{A_0 - A_f}{A_0} \times 100\% \quad (1)$$

where A_0 is the initial radioactivity (counts per minute, cpm) before decontamination and A_f is the final radioactivity (cpm) after decontamination.

On SUS surfaces, 1 h CPU exhibited a higher R (87.2%) than 1 h APU (77.9%), which is attributed to CPU's greater hydrophilicity and stronger affinity for hydrophilic Cs^+ ions (Fig. 2d). In contrast, after 3 h of drying, both CPU (94.9%) and APU (95.0%) showed comparable R. These results are consistent with the SFO removal efficiencies measured by UV-Vis and ICP-TQ-MS analyses (Table S7), demonstrating that PU coatings effectively remove both particulate and ionic contaminants on the surface. Notably, both 3 h CPU and APU outperformed the commercial reference DeconGel (93.8% after 24 h of application), highlighting their potential as faster and more effective alternatives for radioactive cesium decontamination (Fig. 4d).

The rough and porous nature of cement surfaces allows radioactive elements to penetrate deeply into the substrate, thereby reducing removal efficiency. Consequently, achieving effective decontamination on cement remains a significant challenge.[53] To address this issue, the decontamination performance of CPU and APU coatings on cement was compared. Under 1 h drying condition, CPU demonstrated higher removal efficiency than APU, consistent with the trend observed on SUS substrates. Although the removal efficiency of 1 h CPU (5.8%) was slightly lower than that of DeconGel applied for 24 hours (8.4%), the comparable performance achieved in a much shorter time highlights the time-saving advantage of CPU. Specifically, CPU could be applied up to 24 times within the treatment duration required for a single DeconGel application. The 3 h CPU coating exhibited significantly higher removal efficiency (59.1%) than both APU and DeconGel. This enhancement resulted from substrate failure caused by the strong adhesion of CPU, which led to physical stripping of approximately 300 ± 30 μm of the cement surface. Therefore, the 3 h CPU formulation may be unsuitable for applications that require preservation of the substrate. To overcome this limitation and evaluate the feasibility of repeated decontamination using CPU, we developed a "1 h × 2" strategy, wherein the coating was applied and removed twice, each after 1 h of drying. This approach effectively improved removal performance without damaging the cement substrate. The 1 h × 2 CPU achieved the highest removal efficiency on cement (13.1%), followed by 1 h × 2 APU (11.2%) and DeconGel (8.4% after 24 h). These results suggest that 1 h × 2 CPU is a promising alternative to DeconGel for cement surface decontamination. Notably, just two successive applications of the 1 h CPU coating yielded a removal efficiency of 1.48 times greater than that of a single 24 hour DeconGel treatment.

Dissolution and recycling properties

The dissolution behavior of strippable coatings is an important characteristic, as it facilitates post-decontamination handling and may contribute to reducing secondary organic radioactive waste.[56] To evaluate their dissolution behavior, dried coatings were immersed in water, ethanol, and acetone, and their solubility was monitored over time (Fig. S10). Both CPU and APU maintained structural integrity in water and ethanol even after seven days. In contrast, they completely dissolved in acetone within 30 minutes, or within 1 minute under vortex mixing, forming a clear solution.

By comparison, DeconGel began dissolving in water after 3 h and was fully dissolved within 24 h. These results demonstrate that CPU and APU are highly soluble in acetone but insoluble in

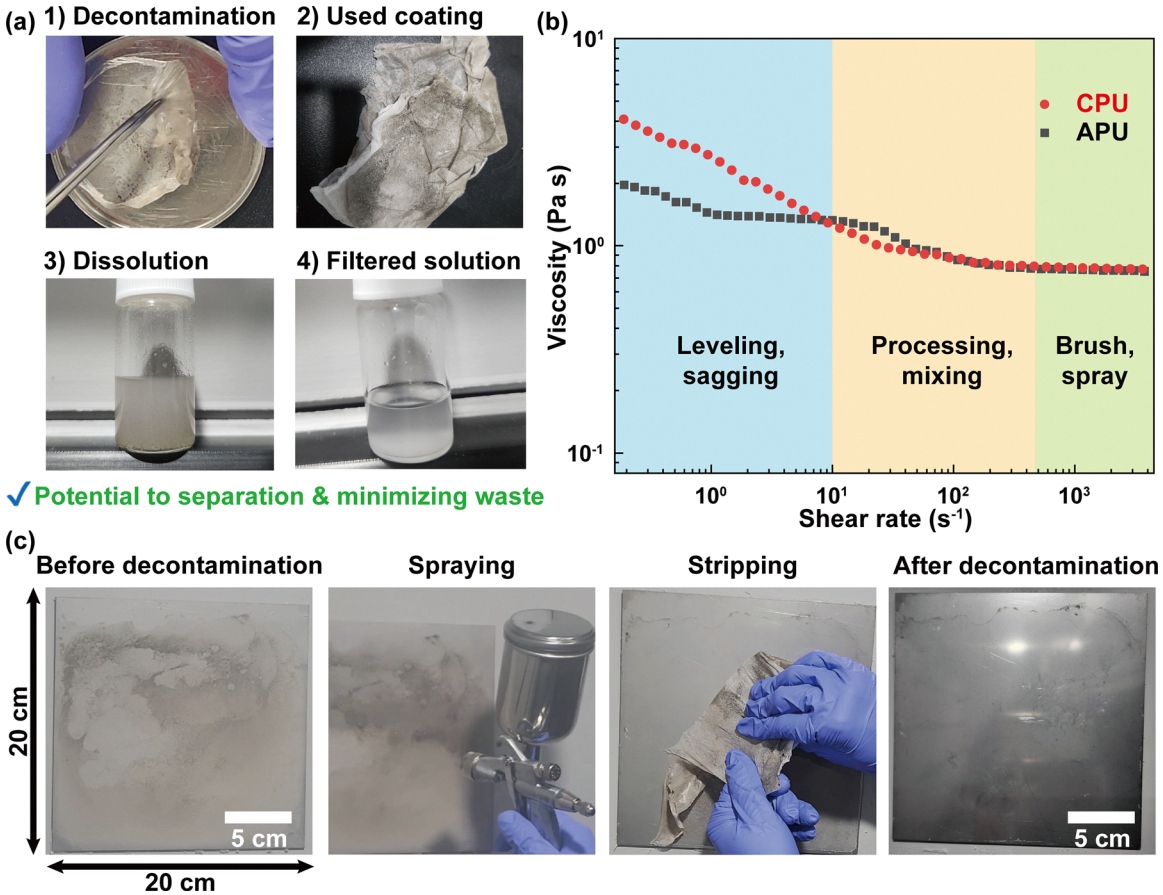

Fig. 5 (a) Separation process of the used CPU by acetone dissolution and filtering. (b) Viscosity changes of strippable PU coatings at different shear rates (0.1–5000 s^{-1}). (c) Process of the spray test using a portable spray system.

water, ensuring stability in wet environments such as rain or groundwater. This insolubility helps prevent unintended leaching and spread of radioactive contaminants following application.

In addition, the solvent-responsiveness of CPU and APU enables their potential use in separation and recycling processes (Fig. 5a). Accordingly, a separation test was performed to assess the feasibility of coating recycling (Fig. S11). When used coatings contaminated with fallout were dissolved in a mixed solvent of acetone and water, a turbid dispersion was formed. A simple filtration using a 0.8 μm syringe filter yielded a clear polyurethane solution. Then, zeolite was added to the contaminated solution as an adsorbent to eliminate dissolved radionuclides,[57] followed by the same separation procedure using a 0.8 μm syringe filter. Notably, separation of fallout and zeolite from the contaminated solution was achieved, as confirmed by the disappearance of the characteristic XRD peaks after filtration (Fig. S12). After this process, a Cs^+ rejection value of 99.9% was achieved relative to the initial contaminated solution, with a waste mass reduction factor (R_m) of 3.4%. The high rejection value of Cs^+, combined with the low rejection of polyurethane, suggests that the PU coatings have the potential to reduce secondary waste and enable material reuse, although this process was a preliminary feasibility test. Further investigation is required to establish a robust separation protocol and to assess the removal efficiency of radioactive contaminants during the solvent-based recycling process.

Spray coating applicability

To evaluate the feasibility of spray-based application, CPU and APU coatings were tested using a commercial portable spray system commonly used for polyurethane materials. The system included a portable spray gun and an air compressor, offering user-friendly operation and enabling rapid deployment. Unlike conventional two-component polyurethane systems, which require specialized dual-viscosity spray equipment and precise flow rate control,[58] CPU and APU offer a simplified process using a single-component formulation, thereby enhancing usability and coating uniformity.

The viscosities of CPU and APU solutions were measured using a rheometer and found to be suitable for high-viscosity spray applications: 0.78 Pa s for CPU and 0.74 Pa s for APU at a shear rate of 1000 s^{-1} (Fig. 5b).[59] Such viscosities support the formation of thick, uniform coatings during spraying while minimizing overspray and splashing, contributing to improved application control.[29] In addition, their shear-thinning behavior allowed the viscosity to increase upon surface contact, effectively preventing dripping or sagging (Table S9).

The spray coating dried and formed a stable film within 1 h. Application of the solution to a 400 cm^2 surface (20 cm × 20 cm) took approximately 2.5 minutes, corresponding to a spray rate of 160 cm^2 min^{-1} (Movie S1). This rate is significantly faster and more scalable than traditional manual application methods such as brushing.

Even on vertical surfaces, the coatings formed uniform layers without signs of flow or sagging during the 3 h drying period, a performance attributed to the combination of high viscosity and shear-thinning behavior. Furthermore, the dried coatings were easily removed by simple manual peeling (Fig. 5c), highlighting their excellent potential for rapid and effective wide-area surface decontamination *via* spray application.

Conclusions

In this study, we successfully developed a strippable polyurethane (PU) coating for efficient radioactive decontamination. The coating dried within 3 h and could be easily peeled off, enabling rapid and residue-free removal of contaminants.

Among the developed formulations, CPU demonstrated superior performance in environments requiring high mechanical strength, thermal stability, and strong adhesion. In the simulated fallout (SFO) test, CPU achieved a cesium (Cs) removal efficiency of 98.4%. In the radioactive isotope (RI) test using ^{137}Cs, CPU also exhibited excellent performance, attributed to its enhanced polymer cohesion, substrate adhesion, and high hydrophilicity.

Notably, CPU coatings achieved 94.9% removal efficiency of ^{137}Cs from stainless steel (SUS) surfaces within 3 h—significantly outperforming the commercial DeconGel, which required ~24 h to reach similar performance. On cement surfaces, CPU showed a higher removal efficiency (59.1%) compared to DeconGel (8.4%).

In addition to decontamination performance, CPU exhibited excellent solvent-responsiveness: it remained stable in water but dissolved rapidly in acetone, facilitating post-decontamination handling and offering potential for recycling, thereby minimizing secondary waste. Moreover, CPU could be uniformly applied using a portable spray system, forming stable, strippable coatings even on vertical surfaces.

Overall, the CPU strippable PU coating offers a rapid, effective, and scalable solution for nuclear decontamination, particularly in time-critical scenarios. Its high performance, ease of application, and potential for waste reduction make it a sustainable and cost-effective alternative to existing commercial coatings for large-scale deployment. In particular, the short drying time enables rapid initial response, which can help mitigate cascading contamination and reduce the overall environmental impact. Beyond radioactive decontamination, this design principle could inspire next-generation strippable polymers for environmental remediation and protective coatings.

Author contributions

Conceptualization: JSL, MB, and DWL. Data curation: JSL, SK, and HY. Formal analysis: JSL, DK, and YJ. Funding acquisition: HY and DWL. Investigation: JSL, DK, HK, and SK. Methodology: JSL, YJ, HK, MB, HY, and DWL. Project administration: HY and DWL. Resources: HY and DWL. Supervision: MB, HY, and DWL. Validation: DK, YJ, and DWL. Visualization: JSL. Writing – original draft: JSL, MB, and DWL. Writing – review and editing: JSL, DK, YJ, HK, SK, MB, HY, and DWL.

Conflicts of interest

The authors declare that they have no known competing financial interests or personal relationships that could have appeared to influence the work reported in this paper.

Data availability

All experimental data, analysis details, and supplementary information (SI) that support the findings of this study are available within the main article and its SI. Supplementary information is available. See DOI: https://doi.org/10.1039/d5mh02005k.

Acknowledgements

This work was funded by the Basic Science Research Program (RS-2023-NR077057 and RS-2023-00242584) through the National Research Foundation (NRF) of Korea and Ministry of Science and ICT. This work was also supported by the Institute of Civil Military Technology cooperation funded by the Defense Acquisition Program Administration and Ministry of Trade, Industry and Energy of Korea government under grant No. 22-CM-BR-14. This study contains the results obtained by using the equipment of UNIST Office of Research Facilities and Training (ResFacT).

References

1 V. Natarajan, M. Karunanidhi and B. Raja, *Environ. Sci. Pollut. Res.*, 2020, **27**, 29812–29823.
2 J. E. Ten Hoeve and M. Z. Jacobson, *Energy Environ. Sci.*, 2012, **5**, 8743–8757.
3 L. Cheng, S. Y. Li, Y. J. Zhang, X. Meng, Y. Wang, S. Wang and K. Y. Wang, *Adv. Funct. Mater.*, 2025, **35**, 2424406.
4 M. H. Paller, G. T. Jannik and R. A. Baker, *J. Environ. Radioact.*, 2014, **131**, 81–88.
5 H. M. Yang, C. W. Park and K. W. Lee, *Prog. Nucl. Energy*, 2018, **104**, 67–74.
6 P. O'Sullivan, J. Nokhamzon and E. Cantrel, *NEA News*, 2010, **28**, 27–29.
7 Z. Liu, Q. Wang, X. Huang and X. Qian, *ACS Omega*, 2022, **7**, 10944–10954.
8 M. Kaminski, C. Mertz, L. Ortega and N. Kivenas, *J. Environ. Chem. Eng.*, 2016, **4**, 1514–1522.
9 S. Amon, A. Jobst, M. Merklein and N. Hanenkamp, *Proc. CIRP*, 2022, **108**, 601–606.
10 A. Gossard, A. Lilin and S. Faure, *Prog. Nucl. Energy*, 2022, **149**, 104255.
11 M. Yang, Z. Li, Y. Wang and X. Lin, *J. Radioanal. Nucl. Chem.*, 2024, **334**, 501–513.

12 J. C. Liu, J. Hu, J. Li, Y. Zhang and X. J. Li, *Prog. Org. Coat.*, 2023, **184**, 107865.
13 H. M. Yang, S. W. Kim, H. J. Kim, G. E. Lee and J. Y. Jang, *Chemosphere*, 2023, **339**, 139617.
14 I. Cetina, *J. Radioanal. Nucl. Chem.*, 2024, **334**, 1093–1106.
15 S. X. Wang and J. H. Waite, *Nat. Rev. Chem.*, 2025, **9**, 159–172.
16 S. Yu and C. Cha, *Macromol. Res.*, 2023, **31**, 427–441.
17 R. X. Liang, H. J. Yu, L. Wang, N. Wang and B. U. Amin, *Adv. Funct. Mater.*, 2021, **31**, 2102621.
18 M. L. Alfieri, L. Panzella and A. Napolitano, *Eur. J. Org. Chem.*, 2024, e202301002.
19 N. Holten-Andersen, A. Jaishankar, M. J. Harrington, D. E. Fullenkamp, G. DiMarco, L. He, G. H. McKinley, P. B. Messersmith and K. Y. C. Lee, *J. Mater. Chem. B*, 2014, **2**, 2467–2472.
20 G. Yan, G. Chen, Z. Peng, Z. Shen, X. Tang, Y. Sun, X. Zeng and L. Lin, *Adv. Mater. Interfaces*, 2021, **8**, 2100239.
21 L. Zhong, J. H. Lei, J. Deng, Z. Y. Lei, L. Lei and X. S. Xu, *Prog. Nucl. Energy*, 2021, **139**, 103854.
22 O. Redy Keisar, V. Nahum, L. Yehezkel, I. Marcovitch, I. Columbus, G. Fridkin and R. Chen, *ACS Omega*, 2021, **6**, 5359–5367.
23 P. G. Wagle, S. S. Tamboli and A. P. More, *Prog. Org. Coat.*, 2021, **150**, 106005.
24 Y.-S. Joo, J.-R. Cha and M.-S. Gong, *Mater. Sci. Eng., C*, 2018, **91**, 426–435.
25 S. L. Phua, L. Yang, C. L. Toh, S. Huang, Z. Tsakadze, S. K. Lau, Y.-W. Mai and X. Lu, *ACS Appl. Mater. Interfaces*, 2012, **4**, 4571–4578.
26 M. Hayashi and F. Tournilhac, *Polym. Chem.*, 2017, **8**, 461–471.
27 P. Kord Forooshani and B. P. Lee, *J. Polym. Sci. Part A: Polym. Chem.*, 2017, **55**, 9–33.
28 M. Kim, J. Park, K. M. Lee, E. Shin, S. Park, J. Lee, C. Lim, S. K. Kwak, D. W. Lee and B.-S. Kim, *J. Am. Chem. Soc.*, 2022, **144**, 6261–6269.
29 P. T. Elliott, M. J. Steffenhagen and J. E. Glass, *J. Coat. Technol. Res.*, 2007, **4**, 341–349.
30 Q. Chen, C. Wang, T. Wang, B. Lei, J. Wang and J. Guo, *J. Pharm. Sci.*, 2025, **114**, 103565.
31 Z. Y. Ye, Y. Zhang, L. A. Hou, M. L. Zhang, Y. Z. Zhu and Y. Yang, *Chem. Eng. J.*, 2022, **446**, 137143.
32 W. Zhang, R. Wang, Z. Sun, X. Zhu, Q. Zhao, T. Zhang, A. Cholewinski, F. Yang, B. Zhao, R. Pinnaratip, P. K. Forooshani and B. P. Lee, *Chem. Soc. Rev.*, 2020, **49**, 433–464.
33 R. K. Chitumalla, K. Kim, X. Gao and J. Jang, *Phys. Chem. Chem. Phys.*, 2021, **23**, 1031–1037.
34 J. Wang, L. Zheng, L. Zhao and T. Zhang, *J. Radioanal. Nucl. Chem.*, 2021, **330**, 29–36.
35 H. Park, D. Lim, G. W. Lee, M. J. Baek and D. W. Lee, *Adv. Funct. Mater.*, 2023, **33**, 2305750.
36 H. Kwon, S. Shin, Y. Yu, W. Lee, H. Park, S. Y. Lee, E. Woo, D. Ahn, M.-J. Baek and D. W. Lee, *Polym. Test.*, 2023, **129**, 108260.
37 B. Chen, K. Lei, D. Zhu, C. Yang, C. Sun, W. Xiao, Z. Zheng and X. Wang, *Adv. Mater. Interfaces*, 2021, **8**, 2100657.
38 R. Guo, Q. Zhang, Y. Wu, H. Chen, Y. Liu, J. Wang, X. Duan, Q. Chen, Z. Ge and Y. Zhang, *Adv. Mater.*, 2023, **35**, 2212130.
39 I. Palle, V. Lodin, A. A. M. Yunus, S. H. Lee, P. M. Tahir, N. Hori, P. Antov and A. Takemura, *Polymers*, 2023, **15**, 1154.
40 H. Wei, J. Xia, W. Zhou, L. Zhou, G. Hussain, Q. Li and K. Ostrikov, *Composites, Part B*, 2020, **193**, 108035.
41 S. V. S. Rao and K. B. Lal, *J. Radioanal. Nucl. Chem.*, 2004, **260**, 35–42.
42 J. H. Lee, M. H. Myung, M. J. Baek, H. S. Kim and D. W. Lee, *Polym. Test.*, 2019, **76**, 305–311.
43 J. H. Lee and D. W. Lee, *Appl. Surf. Sci.*, 2020, **500**, 144246.
44 W. Chen, Z. Wu, X. He, Y. Su, S.-K. Oh and S. Zhang, *Prog. Org. Coat.*, 2024, **186**, 108001.
45 P. H. Donohue, A. Simonetti, E. C. Koeman, S. Mana and P. C. Burns, *J. Radioanal. Nucl. Chem.*, 2015, **306**, 457–467.
46 S. W. Kim, H. M. Yang and H. J. Kim, *Nucl. Eng. Technol.*, 2024, **56**, 5386–5395.
47 M. Długosz-Lisiecka, M. Lopes, A. Monteiro and J. Ferreira, *Sci. Rep.*, 2025, **15**, 24642.
48 H. J. Kim, S. J. Kim, S. Hyeon, H. H. Kang and K. Y. Lee, *ACS Omega*, 2020, **5**, 20261–20269.
49 X. Zhang, P. Gu and Y. Liu, *Chemosphere*, 2019, **215**, 543–553.
50 C. Xu, L. Yuan, X. Shen and M. Zhai, *Dalton Trans.*, 2010, **39**, 3897–3902.
51 P. Winkler, *Concr. Repair Bull.*, 2013, **3**, 17.
52 H. M. Yang, I. H. Yoon and Y. Lee, *Chem. Eng. J.*, 2020, **402**, 126299.
53 X. Xu, X. Pan, J. Li, Z. Li, Y. Xie and X. Lin, *Chemosphere*, 2022, **308**, 136187.
54 Y. Zhu, Y. He, H. Zhang, X. Meng, Y. Liu, S. Chen and X. Men, *Appl. Surf. Sci.*, 2026, **720**, 165345.
55 E. Filippidi, T. R. Cristiani, C. D. Eisenbach, J. H. Waite, J. N. Israelachvili, B. K. Ahn and M. T. Valentine, *Science*, 2017, **358**, 502–505.
56 G. Tochaikul, A. Phattanasub, P. Khemkham, K. Saengtham-thawee, N. Danthanavat and N. Moonkum, *Kerntechnik*, 2022, **87**, 208–225.
57 S. Kwon, C. Kim, E. Han, H. Lee, H. S. Cho and M. Choi, *J. Hazard. Mater.*, 2021, **408**, 124419.
58 L. M. Chen, Z. Hong, W. L. Kwan, C. H. Lu, Y. F. Lai, B. Lei, C. P. Liu and Y. Yang, *ACS Nano*, 2010, **4**, 4744–4752.
59 I. D. A. Mariz, I. S. Millichamp, J. C. de la Cal and J. R. Leiza, *Prog. Org. Coat.*, 2010, **68**, 225–233.

